Neuron
Article

HSP90β Regulates Rapsyn Turnover and Subsequent AChR Cluster Formation and Maintenance

Shiwen Luo,[1] Bin Zhang,[1] Xian-ping Dong,[1] Yanmei Tao,[1] Annie Ting,[1] Zheng Zhou,[1] James Meixiong,[1] Junjie Luo,[1] F.C. Alex Chiu,[1] Wen C. Xiong,[1] and Lin Mei[1,*]
[1]Program of Developmental Neurobiology, Institute of Molecular Medicine and Genetics, Medical College of Georgia, Augusta, GA 30912, USA
*Correspondence: lmei@mcg.edu
DOI 10.1016/j.neuron.2008.08.013

SUMMARY

Rapsyn, an acetylcholine receptor (AChR)-interacting protein, is essential for synapse formation at the neuromuscular junction (NMJ). Like many synaptic proteins, rapsyn turns over rapidly at synapses. However, little is known about molecular mechanisms that govern rapsyn stability. Using a differential mass-spectrometry approach, we identified heat-shock protein 90β (HSP90β) as a component in surface AChR clusters. The HSP90β-AChR interaction required rapsyn and was stimulated by agrin. Inhibition of HSP90β activity or expression, or disruption of its interaction with rapsyn attenuated agrin-induced formation of AChR clusters in vitro and impaired the development and maintenance of the NMJ in vivo. Finally, we showed that HSP90β was necessary for rapsyn stabilization and regulated its proteasome-dependent degradation. Together, these results indicate a role of HSP90β in NMJ development by regulating rapsyn turnover and subsequent AChR cluster formation and maintenance.

INTRODUCTION

Synapses are fundamental units for efficient communication between neurons and their target cells. Despite significant progress in understanding the structure of matured synapses, less is known about the mechanisms by which neurotransmitter receptors are targeted to and anchored at postsynaptic regions (Sanes and Lichtman, 2001; Waites et al., 2005). Increasing evidence suggests that they are mobile, and exchanges occur continually between synaptic and extrasynaptic pools (Akaaboune et al., 1999). This process is regulated by proteins that interact directly with the receptors or indirectly via adaptor proteins. Several such proteins have been identified, including transmembrane AMPAR regulatory proteins (TARPs) for AMPA receptors, PSD-95 for NMDA receptors, homer for mGlu receptors, and gephyrin for GABA receptors (Collingridge et al., 2004; Elias et al., 2006; Waites et al., 2005). Due to easy accessibility and peripheral location, the neuromuscular junction (NMJ) has served as an informative model for synaptogenesis (Sanes and Lichtman, 2001). Synaptic concentration of AChRs is generated by complex interactions between motoneuron terminals and skeletal muscles, resulting in AChR aggregation and local synthesis (Fu et al., 2008; Li et al., 2008; Sanes and Lichtman, 2001; Schaeffer et al., 2001). Neural agrin clusters AChRs via activating the transmembrane tyrosine kinase MuSK (DeChiara et al., 1996; Gautam et al., 1996; Glass et al., 1996; Herbst and Burden, 2000; McMahan et al., 1992; Zhou et al., 1999), whereas ACh is thought to disassemble receptor clusters in nonsynaptic areas via activating muscle fibers (Brandon et al., 2003; Lin et al., 2005; Misgeld et al., 2002). MuSK is also critically involved in the prepatterning of muscles because aneural AChR-rich sites are absent in MuSK knockout mice (Kim and Burden, 2008; Lin et al., 2001). The intracellular pathway downstream of MuSK remains unclear. It is thought to involve the adaptor protein Dok-7 (Okada et al., 2006) and several enzymes, including Src-family kinase (Ferns et al., 1996; Mittaud et al., 2001; Mohamed et al., 2001; Qu and Huganir, 1994; Wallace, 1991), Abl (Finn et al., 2003), geranylgeranyl transferase I (GGT) (Luo et al., 2003), GTPases of the Rho family (Weston et al., 2000, 2003), and Pak1, a serine/threonine kinase that is activated by Rho GTPases (Luo et al., 2002).

Rapsyn is a key cytoplasmic protein in concentrating AChRs at the NMJ (Sanes and Lichtman, 2001). *Rapsyn*$^{-/-}$ mice lack differentiated NMJs and fail to form AChR clusters (Gautam et al., 1995). Rapsyn interacts with the AChR, which is increased by agrin and correlates with cytoskeletal linkage of the AChR (Moransard et al., 2003). Recent evidence suggests that rapsyn regulates AChR clustering by inhibiting the activation of Cdk5 (Chen et al., 2007) and by associating with the β-catenin/α-catenin complex (Zhang et al., 2007). Interestingly, rapsyn turns over rapidly, with a half-life of one to several hours in muscle cells (Bruneau and Akaaboune, 2007; Frail et al., 1989). How the stability of rapsyn is regulated and contributes to AChR clustering and NMJ formation remains unclear.

To study the mechanisms of AChR clustering, we sought to identify proteins that became associated with aggregated surface AChRs in intact muscle cells using a differential proteomic approach. We identified HSP90β, a molecular chaperone implicated in stability and function of client proteins (Pearl and Prodromou, 2006). Its association with surface AChRs was via direct interaction with rapsyn and was increased by agrin. We explored the consequences of inhibiting HSP90β activity or expression and of disrupting its interaction with rapsyn. Results of these experiments indicate a role of HSP90β in NMJ development by regulating rapsyn turnover and subsequent AChR cluster formation and maintenance.

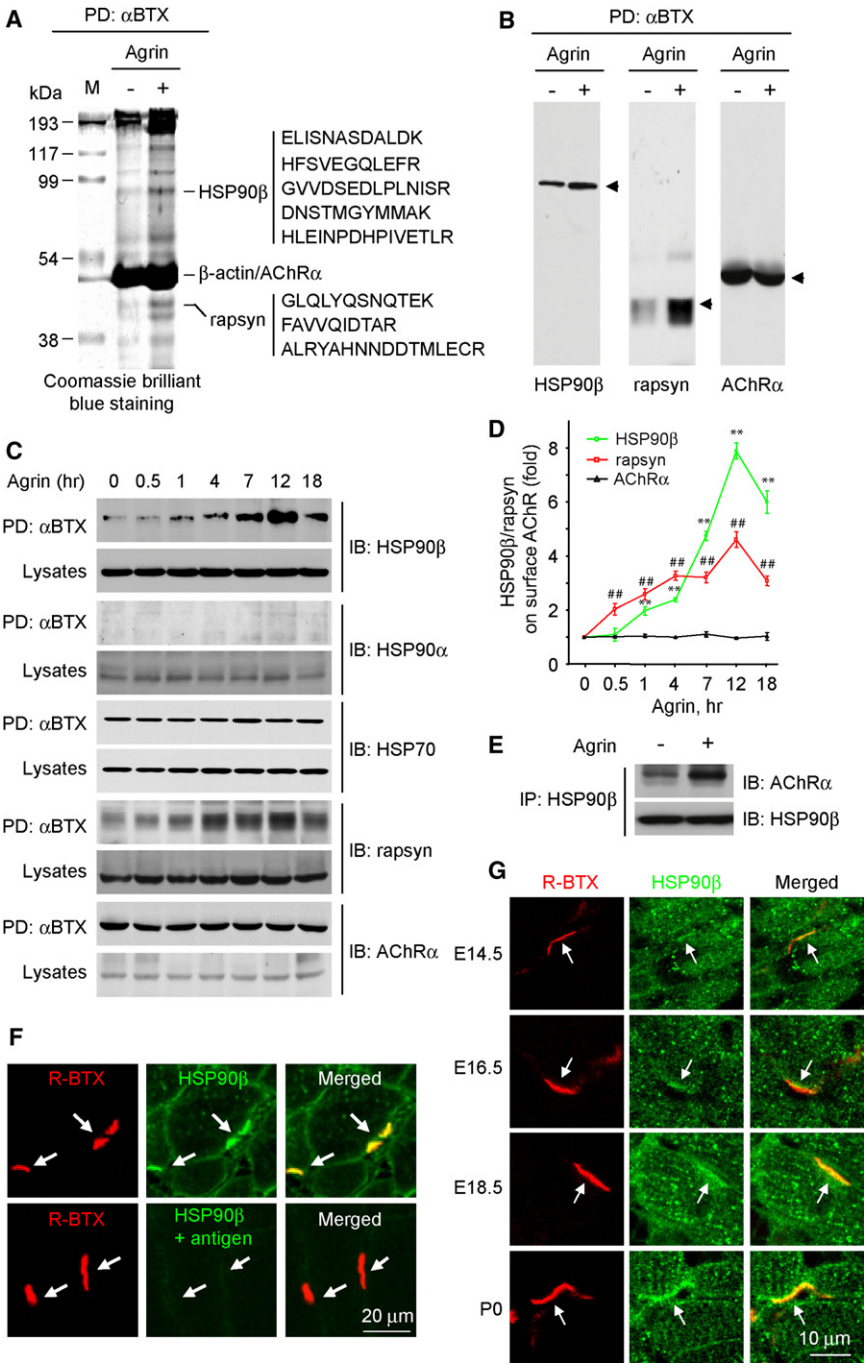

Figure 1. Agrin-Regulated Association of HSP90β with Surface AChRs

(A) Identification of HSP90β as a protein associated with surface-aggregated AChRs. C2C12 myotubes were stimulated without or with agrin for 18 hr. Live myotubes were incubated with 300 nM biotin-αBTX for 2 hr at 4°C to label surface AChR. The AChR complex was purified by streptavidin-coupled agarose beads, resolved by SDS-PAGE and coomassie brilliant blue staining. Distinct bands increased by agrin were subjected to mass spectrometry, which yielded peptide sequences that matched HSP90β and rapsyn.

(B) Immunoblot of AChR-associated proteins by antibodies against HSP90β and rapsyn. AChRα subunit was also blotted to indicate equal amounts.

(C) Time-dependent specific association of HSP90β with surface AChRs. C2C12 myotubes were treated with agrin for different times. Proteins associated with surface AChRs and in lysates were analyzed by immunoblotting with indicated antibodies.

(D) Quantitative analysis of the amounts of HSP90β and rapsyn associated with surface AChRs in (C). Data were shown as mean ± SEM; n = 5; ## and **, $p < 0.01$.

(E) Increased coprecipitation of AChRs and HSP90β in agrin-stimulated myotubes. C2C12 myotubes were stimulated without or with agrin for 12 hr and lysed. Lysates were subjected to immunoprecipitation with anti-HSP90β antibody. Precipitated proteins were probed with indicated antibodies.

(F and G) Enrichment of HSP90β at adult and developing NMJs. Muscle sections of adult mouse tibialis anterior muscles (F) and diaphragms of indicated ages (G) were costained with R-BTX (red), which binds postsynaptic AChRs, and antibody against HSP90β (green, Alexa Fluor 488). In some experiments in (F), the antibody was incubated with the antigen. Arrows indicate colocalization. Scale bar, 20 μm in (F), 10 μm in (G). PD, pull down; IB, immunoblotting; M, protein marker.

RESULTS

Identification of HSP90β in the Complex of Surface AChR Clusters

To understand the mechanisms of AChR clustering, we attempted to identify proteins that are preferentially associated with aggregated versus diffused AChRs. Live, intact C2C12 muscle cells were incubated with biotin-conjugated α-bungarotoxin (αBTX) to label surface AChR following treatment with or without agrin. Receptor-associated proteins were purified by streptavidin-coupled agarose beads, resolved by SDS-PAGE, and identified by mass spectrometry. This led to the identification of several proteins, including HSP90β and rapsyn, a protein known to interact with AChR upon agrin stimulation (Figures 1A and 1B) (Moransard et al., 2003). HSP90β is a chaperone ATPase of the HSP90 family implicated in protein maturation and targeting. Expression of HSP90β is not inducible with stress, unlike HSP90α, whose level increases in cells under stress. HSP90α was not detectable in surface AChR complexes regardless of agrin stimulation (Figure 1C), demonstrating the specificity of the interaction between HSP90β and surface-aggregated AChR. Moreover, the HSP90β association was time dependent, peaking (~8-fold above basal) around 12 hr after agrin

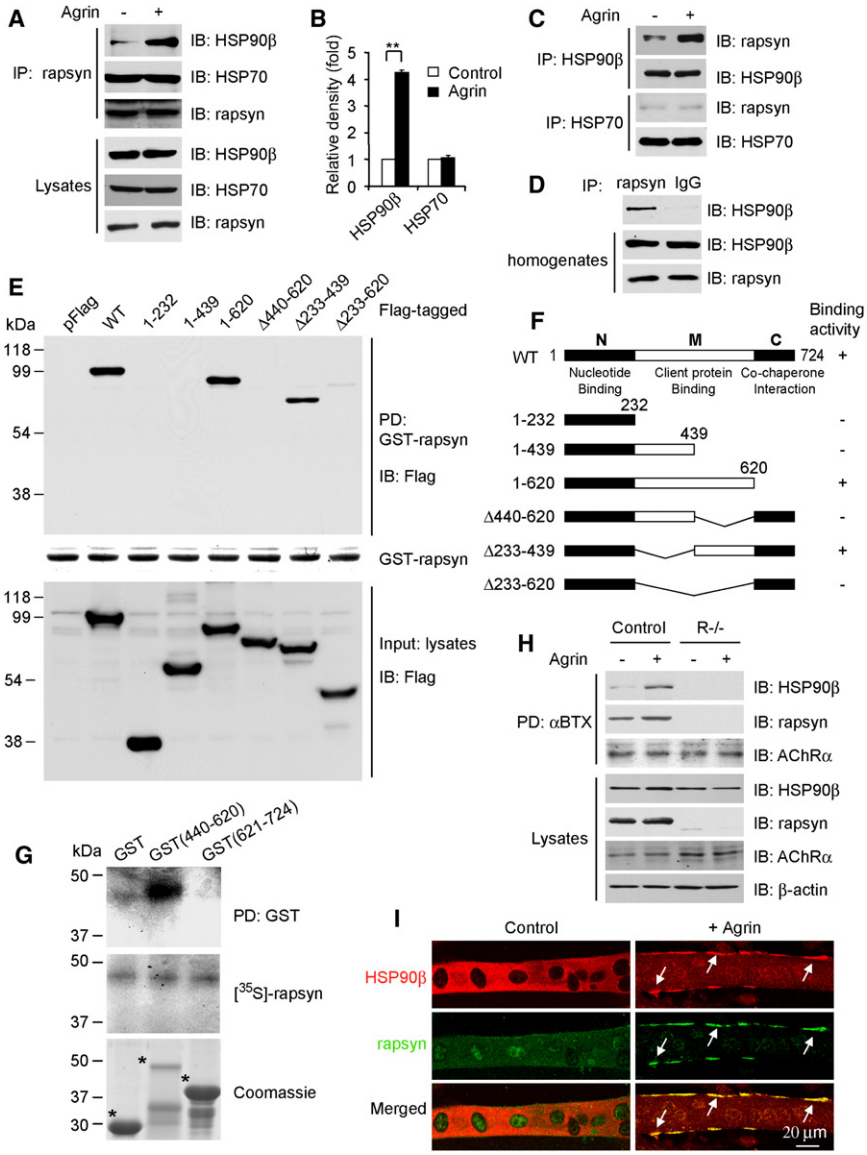

Figure 2. Interaction of Rapsyn with HSP90β in Cultured Cells and Muscle Tissue

(A) Increased rapsyn-HSP90β interaction in agrin-stimulated myotubes. Myotubes were stimulated with agrin for 12 hr and resulting lysates were subjected to immunoprecipitation of rapsyn. Precipitated proteins were probed using indicated antibodies.

(B) Quantitative analysis of the amounts of HSP90β associated with rapsyn in (A). Data were shown as mean ± SEM; n = 5; $^{**}p < 0.01$.

(C) Coprecipitation experiments were done as in (A) except anti-HSP90β and HSP70 antibodies were used in immunoprecipitation. Precipitated proteins were probed using indicated antibodies.

(D) Interaction of HSP90β with rapsyn in mouse muscles. Mouse muscle homogenates were incubated with anti-rapsyn antibody or rabbit normal IgG. Precipitates were probed for HSP90β. Homogenates were also probed for HSP90β and rapsyn (bottom panels).

(E) Identification of HSP90β domains for rapsyn interaction. Bacterial GST-rapsyn, immobilized on glutathione-Sepharose 4B beads, was incubated with lysates from HEK293 cells expressing Flag-HSP90β constructs in (E). Precipitated proteins (PD) and input lysates were immunoblotted (IB) with anti-Flag antibody.

(F) HSP90β constructs and rapsyn binding activity.

(G) Direct interaction between HSP90β and rapsyn. [^{35}S]-labeled rapsyn protein was generated by in vitro translation (middle panel) and incubated with bacterial GST or GST fusion proteins containing HSP90β (440–620 or 621–724), which were immobilized on glutathione-Sepharose 4B beads (bottom panel, *). Bead-associated [^{35}S]-rapsyn was resolved by SDS-PAGE and visualized by autoradiogram (top panel).

(H) Rapsyn-dependent association of HSP90β to surface AChRs. Control and rapsyn deficient (R−/−) myotubes were stimulated without or with agrin for 12 hr. The surface AChR complex was purified as in Figure 1 and probed with indicated antibodies.

(I) Colocalization of HSP90β and rapsyn in C2C12 myotubes. C2C12 myotubes were treated with or without agrin for 12 hr. The samples were fixed and costained with antibodies against HSP90β (Alexa Fluor 594, red) and rapsyn (Alexa Fluor 488, green). Images were acquired by using a Zeiss confocal microscope. Arrow indicates colocalization. Scale bar, 20 μm.

stimulation (Figures 1C and 1D), a time when induced AChR clusters are detectable. Note that levels of HSP90β and surface AChR remained unchanged under these conditions (Figure 1C). In agreement, the amount of AChR was increased in HSP90β precipitates in reciprocal experiments (Figure 1E). HSP90β immunoreactivity showed a pattern similar to that of rhodamine-conjugated αBTX (R-BTX) staining in developing and adult muscles (Figures 1F and 1G), but not in spontaneous clusters in cultured myotubes (Figure S1B available online), suggesting that HSP90β is enriched at the NMJ. These observations reveal that HSP90β associates with surface AChRs upon agrin stimulation. HSP70 also associated with surface AChRs. However, this association did not appear to be regulated by agrin (Figure 1C).

HSP90β Associates with AChR via Rapsyn

Next, we examined whether rapsyn associates with HSP90β in a manner dependent upon agrin stimulation. Immunoprecipitation with an anti-rapsyn antibody (Figure S2) brought down HSP90β, and the coprecipitation was increased in agrin-stimulated cells (Figures 2A and 2B). In reciprocal experiments, more rapsyn coprecipitated with HSP90β upon agrin stimulation (Figure 2C). Moreover, the rapsyn-HSP90β association was detectable in mouse muscle homogenates (Figure 2D), suggesting in vivo interaction of the two proteins. Intriguingly, rapsyn could also interact with HSP70 in an agrin-independent manner (Figures 2A and 2C). In domain mapping experiments, GST-rapsyn was able to pull down wild-type and truncation mutant HSP90β1-620 (Figure 2E), suggesting that the C-terminal region

could be dispensable for the interaction. Deletion of aa 440–620, however, prevented HSP90β from interacting with rapsyn, suggesting the necessity of this region (Figures 2E and 2F). Moreover, a GST fusion protein containing aa 440–620 was able to interact with [^{35}S]-labeled rapsyn generated by in vitro translation (Figure 2G), suggesting that aa 440–620 is sufficient for interaction. This result also demonstrated that the interaction between HSP90β and rapsyn is direct. Rapsyn has three domains: TPR domains for self-association, a coiled-coil domain for interaction with AChR, and a Ring domain for interaction with β-dystroglycan (Bartoli et al., 2001). The TPR domains appeared to be necessary and sufficient for interaction with HSP90β (Figure S3).

Direct interaction between HSP90β and rapsyn could suggest that HSP90β may associate indirectly with surface AChRs, i.e., via rapsyn. This hypothesis predicts that AChR is not associated with HSP90β in the absence of rapsyn. To test this, we used muscle cells derived from rapsyn mutant mice (clone 11-7) that are deficient in rapsyn and do not form AChR clusters in response to agrin (Apel et al., 1997; Fuhrer et al., 1999). As shown in Figure 2H, rapsyn as well as HSP90β became associated with surface AChRs in agrin-stimulated control muscle cells (clone 12-10) derived from heterozygous littermates. In contrast, however, HSP90β was barely detectable in surface AChRs in *rapsyn*$^{-/-}$ myotubes (Figure 2H). Similarly, AChR was not detectable in precipitates of HSP90β in *rapsyn*$^{-/-}$ cells (Figure S4). Note that levels of HSP90β and AChR were similar between control and *rapsyn*$^{-/-}$ myotubes. These results demonstrate the dependence of the HSP90β-AChR association on rapsyn and that agrin stimulates the interaction between rapsyn and HSP90β. In support of this, HSP90β and rapsyn were colocalized in agrin-stimulated C2C12 myotubes (Figure 2I) and the developing NMJ (Figure S1A).

Inhibition of HSP90β Attenuates AChR Cluster Formation In Vitro and In Vivo

To investigate the function of HSP90β in AChR clustering, muscle cells were treated with 17-(allylamino)-17-demethoxygeldanamycin (17-AAG), an inhibitor of HSP90 (Sharp and Workman, 2006). It inhibits the ATPase activity by binding to the N-terminal region and thus alters the conformation of HSP90β and the chaperone complex (Stebbins et al., 1997). 17-AAG (5 μM, 12 hr) had no apparent effect on myotube viability or morphology of C2C12 myotubes (data not shown). However, it inhibited agrin-induced formation of AChR clusters in a dose-dependent manner (Figure 3A) without altering the levels of surface AChR (Figure 3B), MuSK, or its activation by agrin or c-Abl, Rac, or Cdc42 (Figures 3C and 3D). A similar inhibitory effect was observed in myotubes pretreated with 17-AAG (Figure S5). Intriguingly, 17-AAG (0.1 μM, 12 hr) dramatically reduced the amount of rapsyn associated with surface AChRs without significant changes of that in lysates, while at increased concentrations the amount of rapsyn in lysates was reduced (Figures 3B and 3E). These results suggest a role for HSP90β in promoting rapsyn stability (see below). Concomitantly, the amount of HSP90β in the AChR complex, but not in lysates, was reduced (Figure 3B). These results suggest that inhibition of HSP90β attenuates its interaction with rapsyn and thus reduces the latter's stability, and subsequently, AChR cluster formation is compromised. Consistent with this model, the stability of AChR clusters in 17-AAG-treated muscle cells was reduced, with a half-life of about 4 hr in comparison with that of 7–12 hr in control cells (Figure 3F) (Camilleri et al., 2007; Kim and Nelson, 2000; Wallace, 1988; Zhu et al., 2006). Time-lapse imaging indicated that 17-AAG treatment increased the rate of disappearance of AChR aggregates (Figure S6). Thus, HSP90β may regulate both the formation and maintenance of AChR clusters.

We determined the role of HSP90β in NMJ formation in vivo by injecting 17-AAG intraperitoneally into embryos in utero at E14.5, a time when the NMJ starts to form (Lin et al., 2001; Zhu et al., 2006). Diaphragms were whole-mount stained with antibodies against synaptophysin and neurofilament to label phrenic nerve branches and terminals and with R-BTX to label the AChR. As shown in Figure 4, 17-AAG decreased the number and size of AChR clusters (Figures 4A and 4A′) and reduced rapsyn immunoreactivity (Figure 4B), consistent with the notion that HSP90β regulates rapsyn stability and thus AChR cluster formation in vivo. Phrenic nerve branches and terminals were apparently similar in control and 17-AAG-treated muscles (Figure 4A). Due to the decrease in AChR clusters, numerous nerve terminals did not costain with R-BTX (arrow, Figure 4A′), unlike control diaphragms where almost all terminals were associated with AChR clusters (arrowhead, Figure 4A′). Note that 17-AAG injection reduced rapsyn levels in muscles (mostly in the synaptic region, Figures S7A and S7B) but had no apparent effect on the morphology of muscles, thickness of diaphragms, or size of muscle fibers (Figure S8A). No effect was observed on the morphology or number of motoneurons (Figure S8B) or distribution of ACh esterase (AChE), an enzyme enriched in the synaptic cleft of the NMJ (Figure S8C). These results suggest a role of HSP90β in NMJ formation. To determine whether it is also involved in NMJ maintenance, 17-AAG was injected intraperitoneally into P7, P14, and P30 mice, which reduced rapsyn in muscles (Figure S9A) but had no apparent effect on muscle fiber morphology or size (Figure S9B). Unlike NMJs in control mice that appeared like "pretzels" (Figure 4C), AChR clusters in 17-AAG-treated mice were disrupted. Quantitatively, the number of uninterrupted AChR cluster fragments was increased, whereas the area of each fragment, area of each NMJ, and intensity of AChR clusters were reduced in muscles of 17-AAG-treated mice (Figure 4D). The effect was age dependent, more severe in P7 mice. Consistent with biochemical and morphological deficits, 17-AAG-injected P7 and P14 mice showed a reduction in step length (Figure S10). These data indicate a role of HSP90β in AChR cluster maintenance. Together with observations that HSP90β inhibition attenuates AChR clustering in cultured muscle cells, these observations provide evidence for a role of HSP90β in postsynaptic differentiation at the NMJ.

Repression of HSP90β Expression Inhibits AChR Clustering

To investigate specifically the role of HSP90β, we generated HSP90β miRNA constructs that inhibited HSP90β expression, among which 90β-1205 and 90β-1626 were most effective (Figure 5A). By contrast, HSP90β expression was not affected by a vector that encodes random sequences (control) or LacZ-miRNA. HSP90β-miRNA constructs were introduced into C2C12 myotubes to avoid possible interference with muscle

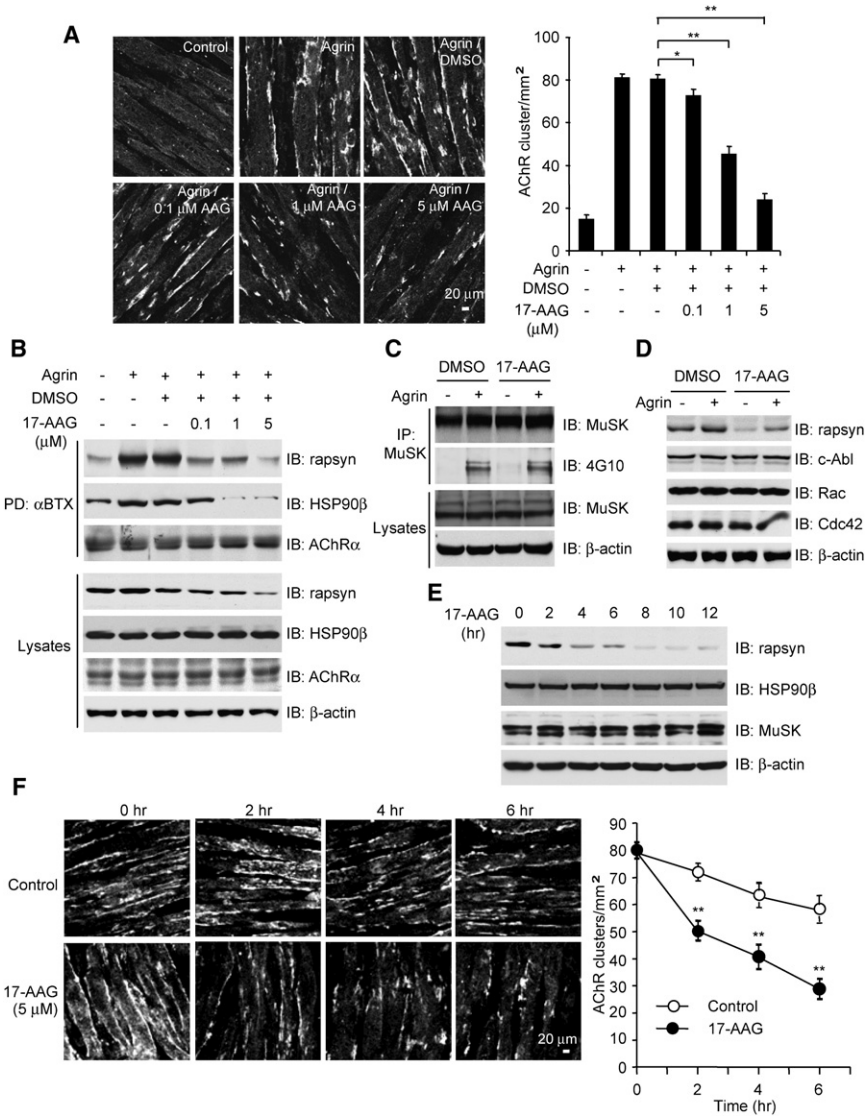

Figure 3. 17-AAG Reduced AChR Cluster Formation and Maintenance in C2C12 Muscle Cells

(A) Inhibition of agrin-induced AChR cluster formation by 17-AAG. C2C12 myotubes were treated without or with agrin in the presence of the vehicle DMSO or 17-AAG at different concentrations. AChR clusters were assayed 12 hr later. Histograms show mean ± SEM; n = 20 in each group; *$p < 0.05$, **$p < 0.01$. Scale bar, 20 μm.

(B) Reduced HSP90β association to surface AChRs in 17-AAG-treated muscle cells. The AChR complex was purified as in Figure 1 from control and treated C2C12 myotubes and probed for rapsyn, HSP90β, and AChR. Lysate input was also probed for the indicated proteins.

(C and D) No effect of 17-AAG on MuSK expression or activation by agrin (C) or expression of c-Abl, Rac, or Cdc42 (D). C2C12 myotubes were treated with or without 5 μM 17-AAG for 1 hr in (C) and for 12 hr in (D). MuSK was immunoprecipitated and probed for phospho-tyrosine using 4G10 antibody (C). Lysates were also probed for the indicated proteins (C and D).

(E) Time-dependent reduction of rapsyn in lysates of 17-AAG (5 μM) treated muscle cells.

(F) Decreased stability of AChR clusters in myotubes treated with 17-AAG. C2C12 myotubes were stimulated with agrin for 12 hr to induce AChR clusters. Cells were washed and switched to a medium without agrin in the presence or absence of 5 μM 17-AAG for indicated times. Histograms show mean ± SEM; n = 10 per group; **$p < 0.01$. Scale bar, 20 μm.

differentiation. Agrin-induced AChR clusters were analyzed in myotubes labeled by GFP, which was encoded by the miRNA vector. As shown in Figure 5C, AChR clustering was markedly attenuated in myotubes transfected with 90β-1205 and 90β-1626, in comparison with control. This effect was specific, as AChR clusters were not affected by 90α-2172 that suppressed HSP90α expression (Figures 5B and 5C). These results corroborate those from studies with the HSP90 inhibitor 17-AAG and demonstrate a role of HSP90β, not HSP90α, in agrin-induced AChR cluster formation in living myotubes.

To repress HSP90β expression in vivo, 90β-1205 DNA was delivered to tibialis anterior muscles of P14 mice by injection and subsequent electroporation, which enabled 67% muscle fibers to express GFP (Figure S11). As shown in Figure 5D, 90β-1205 specifically repressed in vivo expression of HSP90β that was associated with decreased levels of rapsyn 2 weeks after electroporation. AChR clusters were examined in teased individual muscle fibers that express GFP. To ensure that AChRs under examination were formed in muscle fibers that expressed 90β-1205, we reconstructed 3D images of injected muscle fibers. Only clusters on GFP-expressing fibers, as indicated by lateral view of reconstructed 3D images (Figure 5E), were subjected to analysis and quantification. In comparison with control muscles, 90β-1205 disrupted AChR clusters in vivo. AChR clusters became fragmented, with reduced areas of individual fragments and of individual NMJs in 90β-1205-treated muscles (Figures 5E and 5F). The intensity of AChR clusters was also reduced (Figure 5F). Although 90α-2172 reduced levels of HSP90α in electroporated muscles, it had no detectable effect on rapsyn levels or in vivo AChR clustering (Figures 5D–5F). These data indicate that HSP90β, not HSP90α, is involved in AChR cluster maintenance.

Inhibition of AChR Clustering by an HSP90β Mutant

Next, we used a dominant-negative approach to investigate whether AChR clusters require the interaction of HSP90β and rapsyn. We reasoned that HSP90β1-620, a fragment that contains the domain for rapsyn interaction, may prevent endogenous rapsyn from interacting with HSP90β. As shown in Figure 6A, expression of Flag-HSP90β1-620 reduced levels of rapsyn in transfected muscle cells, presumably by disrupting

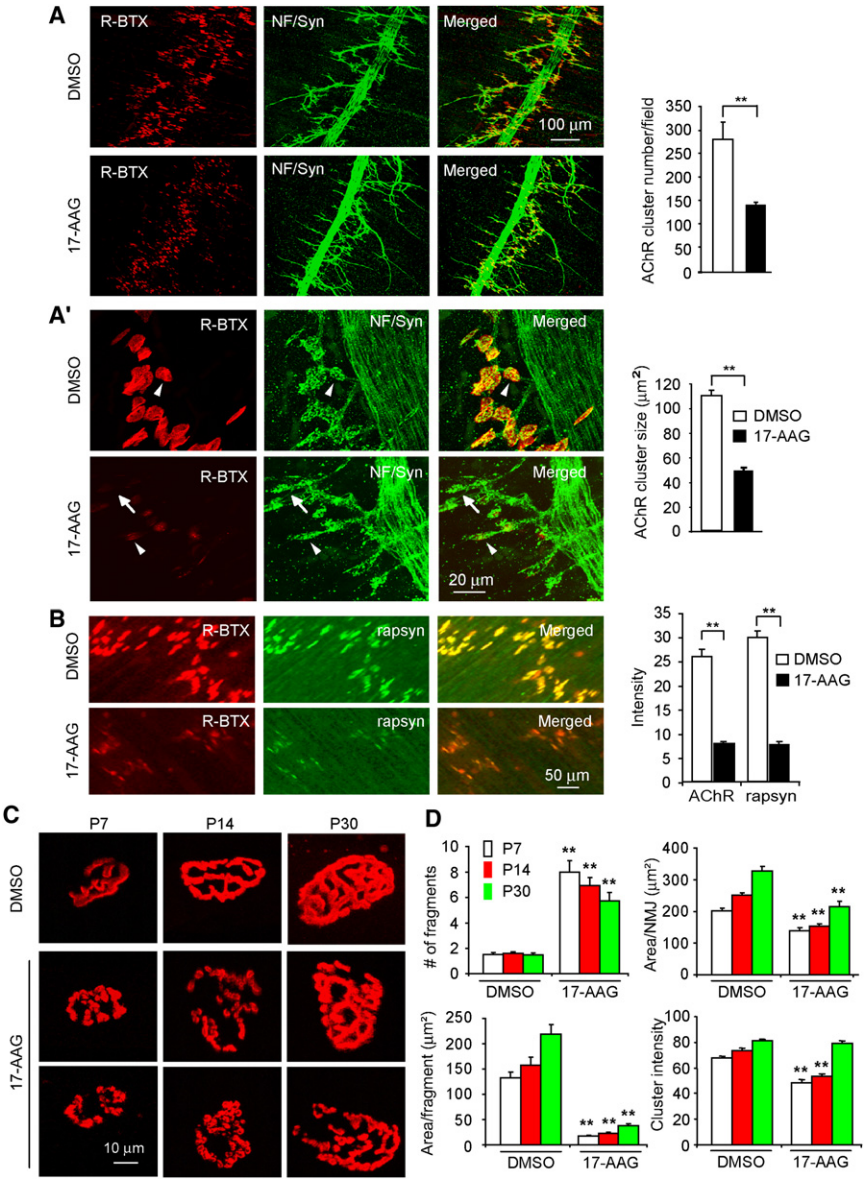

Figure 4. Inhibition of HSP90β Impaired NMJ Formation In Vivo

(A, A′, and B) Mouse embryos (E14.5) in uterus were injected intraperitoneally with 17-AAG (10 μl, 0.5 μM in 10% DMSO) or DMSO (control) daily for 2 days. Diaphragms were dissected at E17.5 and stained whole-mount with R-BTX and antibodies against neurofilament (NF) and synaptophysin (Syn) (A and A′) or rapsyn (B). Collapsed images of diaphragms were captured by a Zeiss confocal laser-scanning microscope. AChR clusters were traced around the perimeters to calculate the area using LSM 5 Image Examiner software (Zeiss). Histograms in (A and A′) show mean ± SEM, n = 6–10 mice for each treatment; **p < 0.01. Arrowhead indicates clusters with both pre- and postsynaptic markers. Arrow indicates a cluster stained for presynaptic markers, but not R-BTX. Histograms in (B) were results of analysis of digitized images using NIH Image 1.63. The mean pixel value (mpv) of each cluster was used to calculate the fluorescence intensity, with background subtracted. Data were shown as mean ± SEM; n = at least 6 mice for each treatment; **p < 0.01.

(C) Mice were injected intraperitoneally at P7, P14, and P30 with 50 μl of 17-AAG (2.5 mg/kg) or DMSO (control) three times a week on alternate days for 2 weeks. AChR clusters were visualized in single teased fibers of tibialis anterior muscles, and Z serial images were collected and collapsed into a single image.

(D) Quantitative analysis of the numbers of R-BTX-positive fragments, areas occupied by individual fragments, areas occupied by individual NMJs, and cluster intensity. Data shown were mean ± SEM, n = 30 AChR clusters of 6 mice of each group (**p < 0.01).

the interaction between rapsyn and endogenous HSP90β. Remarkably, it inhibited agrin-induced AChR clusters in a manner that required the 440-620 domain that interacts with rapsyn. HSP90β constructs harboring this domain (1-620 and Δ233-439), but not those without this domain (1-232, 1-439, Δ440-620, and Δ233-620), were able to inhibit AChR clustering (Figure 6B). These results indicate that the HSP90β-rapsyn interaction may be involved in AChR cluster formation in muscle cells.

To disrupt the interaction in vivo, HSP90β1-620 was subcloned into pIRES2-EGFP to generate pIRES2-(1-620) that expresses EGFP and HSP90β1-620 as two individual proteins (Figure 6C). As shown in Figure 6E, HSP90β1-620 expression reduced rapsyn levels in injected muscles by 40%. AChR clusters were disrupted in HSP90β(1-620)-expressing muscle fibers, but not those expressing EGFP alone (Figure 6D). The number of AChR-positive fragments per NMJ was increased with reduced surface areas of each fragment and individual NMJ. These results, in good agreement with studies of AChR clusters in cultured myotubes (Figure 6B), indicate that disruption of the rapsyn-HPS90β interaction attenuates AChR clustering in vivo. Together with in vivo miRNA experiments, they provide strong evidence for an in vivo role of HSP90β in AChR clustering and NMJ formation.

HSP90β Stabilizes Rapsyn and Regulates Proteasome-Dependent Degradation

Rapsyn is a dynamic protein in the AChR complex with a half-life of one to several hours (Bruneau and Akaaboune, 2007; Frail et al., 1989). The direct interaction between rapsyn and HSP90β may therefore regulate rapsyn stability. To test this hypothesis, we examined effects of 17-AAG on rapsyn stability in C2C12 myotubes in the presence of cycloheximide (CHX) to inhibit translation. As shown in Figure 7A, 17-AAG (5 μM) treatment promoted rapsyn degradation. The half-life of rapsyn decreased by 60% in treated muscle cells (6.1 ± 0.35 hr and 2.4 ± 0.15 hr in control and 17-AAG treated cells, respectively, $p < 0.001$, n = 7).

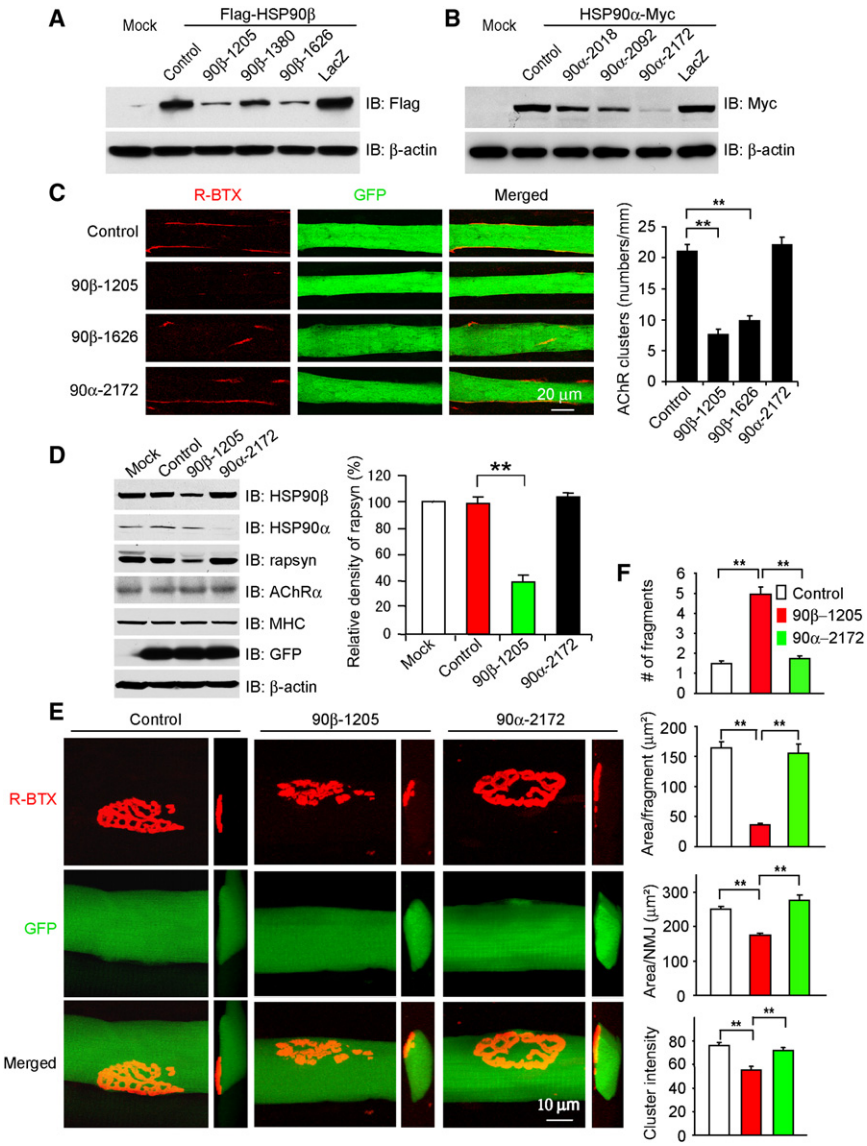

Figure 5. Repression of HSP90β, but Not HSP90α, Expression Impaired Agrin-Induced AChR Clustering In Vitro and In Vivo

(A and B) Inhibition of HSP90β and HSP90α expression by respective miRNA constructs. HEK293 cells were transfected with Flag-HSP90β (A) or Myc-HSP90α (B) along with indicated miRNA constructs of HSP90β (A) or HSP90α (B). The control miRNA encodes scrambled sequences, whereas LacZ encodes miRNA for LacZ. Thirty-six hours after transfection, cell lysates were immunoblotted with antibodies against Flag (A), Myc (B), or β-actin (A and B) for loading control.

(C) Agrin-induced AChR clusters were reduced in myotubes expressing 90β-1205 or 90β-1626, but not 90α-2172. Young C2C12 myotubes were transfected with the control vector (scrambled) and indicated miRNA constructs and stimulated with agrin 24 hr later for 12 hr. AChR clusters were examined in myotubes expressing GFP that was encoded by the miRNA parental vector. Right panel shows quantitative analysis (mean ± SEM, n = 20 each group; $^{**}p < 0.01$).

(D) Decreased rapsyn levels in 90β-1205-expressing, but not 90α-2172-expressing, muscles. Indicated miRNA or control (scrambled) constructs were injected into tibialis anterior muscles of P14 mice. The injected muscles were subjected to electroporation. Fourteen days later, tibialis anterior muscles were homogenized and analyzed by immunoblotting with the indicated antibodies. Shown were representative blots and histograms of quantitative analysis (mean ± SEM, n = 5; $^{**}p < 0.01$).

(E) Fragmentation of AChR clusters in 90β-1205-expressing muscle fibers. miRNA or control constructs were injected as described in (D) into tibialis anterior muscles of P14 mice. AChR clusters were examined 2 weeks later in teased individual muscle fibers that express EGFP alone or EGFP and respective miRNA constructs. AChR clusters were visualized in single teased fibers, and Z serial images were collected and collapsed into a single image. Lateral view of the reconstructed 3D images was shown on the right.

(F) Quantitative analysis of data in (E). Data shown were mean ± SEM, n = 30 AChR clusters of 6 mice of each group ($^{**}p < 0.01$). Scale bar, 10 μm.

The reduction in rapsyn half-life could be attenuated by agrin (Figure 7A), which stimulates the HSP90β-rapsyn interaction (Figures 2A and 2C). 17-AAG at the same concentrations was able to disrupt the HSP90β-rapsyn interaction in a time-dependent manner. The interaction was reduced within 20 min of and almost abolished 60 min after 17-AAG treatment (Figure 7B). Note that the effect of 17-AAG on rapsyn levels in lysates was also time dependent. 17-AAG (5 μM) had little effect on rapsyn levels within 60 min of treatment (Figure 7B), but reduced them significantly 12 hr after (Figures 3B and 3E). These results suggest that rapsyn stability was enhanced by interaction with HSP90β. This notion was supported by further studies with HSP90β-miRNA that reduced rapsyn in transfected cells (Figure 7C). Moreover, expression of HSP90β1-620, a deletion mutant that disrupts the HSP90β-rapsyn interaction, reduced rapsyn levels in a dose-dependent manner (Figure 6A).

Degradation of HSP90 client proteins is thought to be mediated by the 26S proteasome. As such, we investigated whether this system is involved in regulating rapsyn stability. Muscle cells were treated with MG-132, an inhibitor of the 26S proteasome, and rapsyn stability in control and 17-AAG-treated cells was characterized. As shown in Figure 7D, 17-AAG-induced degradation of rapsyn was attenuated by MG-132, but not by lysosomal protease inhibitors chloroquine or monensin. These results suggest that rapsyn undergoes degradation by 26S proteasomes. Consistent with this observation, MG-132 was able to attenuate the inhibitory effect of 17-AAG on AChR cluster formation (Figure 7E). Moreover, overexpression of rapsyn was able to attenuate the inhibitory effect of 17-AAG on AChR clusters (Figure 7F), suggesting the regulation of rapsyn levels could be a mechanism of action of HSP90β. Together, these results indicate that HSP90β was a synaptic chaperone that regulates the

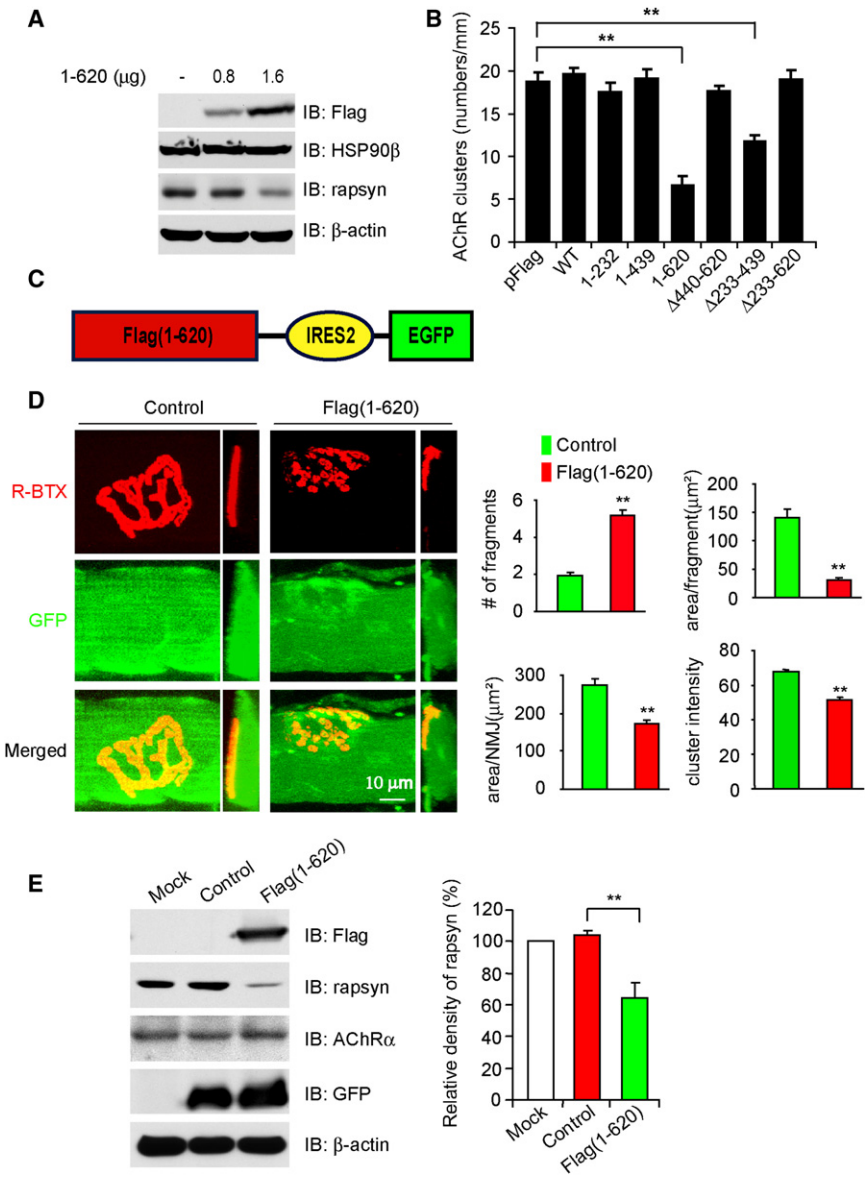

Figure 6. Expression of a HSP90β Mutant Inhibited AChR Clustering

(A) Rapsyn levels were reduced in muscle cells expressing the HSP90β mutant 1-620. C2C12 myotubes were transfected without or with two doses of Flag(1-620). Thirty-six hours after transfection, cells were lysed and resulting lysates were blotted with indicated antibodies.

(B) Inhibition of agrin-induced AChR clustering by HSP90β mutants. C2C12 myotubes were transfected with Flag-HSP90β constructs. Thirty-six hours after transfection, AChR clusters were assayed in Flag-positive myotubes. Data are shown as mean ± SEM, n = 20 each group; $^{**}p < 0.01$.

(C) Schematic diagram of the pIRES2-HSP90β1-620.

(D) Fragmentation of AChR clusters in HSP90β1-620-expressing muscle fibers. pIRES2-Flag(1-620) or the parental vector was injected into tibialis anterior muscles of P14 mice. The injected muscles were subjected to electroporation. AChR clusters were examined 2 weeks later in teased individual muscle fibers that express EGFP alone or EGFP and HSP90β1-620. Lateral view of the reconstructed 3D images was shown on the right. Quantitative analysis of data was shown in the histograms on the right (mean ± SEM, n = 23 for EGFP [45 fragments] and n = 20 for HSP90β1-620 [103 fragments] from 6 mice; $^{**}p < 0.01$).

(E) Decreased rapsyn levels in HSP90β1-620-expressing muscles. Muscles injected with pIRES2-EGFP vector (control) or pIRES2-Flag(1-620) were homogenized and analyzed for expression of indicated proteins. Quantification of data was shown as mean ± SEM (n = 4; $^{**}p < 0.01$).

stability of rapsyn and subsequently AChR clustering and NMJ formation.

DISCUSSION

Utilizing a proteomic approach, we identified HSP90β as a protein that becomes associated with surface AChR in agrin-stimulated muscle cells. We demonstrate that HSP90β does not interact with the AChR directly; instead, via direct interaction with rapsyn, HSP90β becomes associated with clustered AChR. Consistently, HSP90β is enriched at the NMJ and in AChR clusters in muscle cells. We show that HSP90β regulates AChR clustering. First, treatment of muscle cells with 17-AAG, an HSP90 inhibitor that disrupts the AChR-HSP90β complex, attenuated agrin-induced AChR clustering. 17-AAG also reduced the stability of AChR clusters. Second, suppression of HSP90β expression inhibits agrin-induced AChR clustering in muscle cells. Third, disruption of the HSP90β-rapsyn interaction by a dominant-negative approach inhibits AChR clustering. Mouse embryos injected with 17-AAG form fewer AChR clusters, suggesting that HSP90β is involved in NMJ formation in vivo. Finally, we provide evidence that HSP90β regulates rapsyn stability. Rapsyn was reduced in muscle cells treated with 17-AAG, cells expressing HSP90β-miRNA that suppress HSP90β expression, and cells transfected with HSP90β1-620 that disrupts the interaction of endogenous HSP90β and rapsyn. These results support a working model where agrin stimulates the interaction between HSP90β and rapsyn and thus stabilizes rapsyn. When HSP90β is inhibited or its expression suppressed, rapsyn becomes unstable and degraded possibly via the 26S proteasome system. HSP90β was concentrated at the NMJ (Figures 1F and 1G) and present in agrin-induced AChR clusters (Figure 3B). However, little HSP90β was detectable in spontaneous AChR clusters (Figure S1B), although its association with surface AChR and rapsyn could be demonstrated in naive muscle cells in pull-down and coimmunoprecipitation assays (Figures 1C and 2A). These results could suggest that the amount of HSP90β

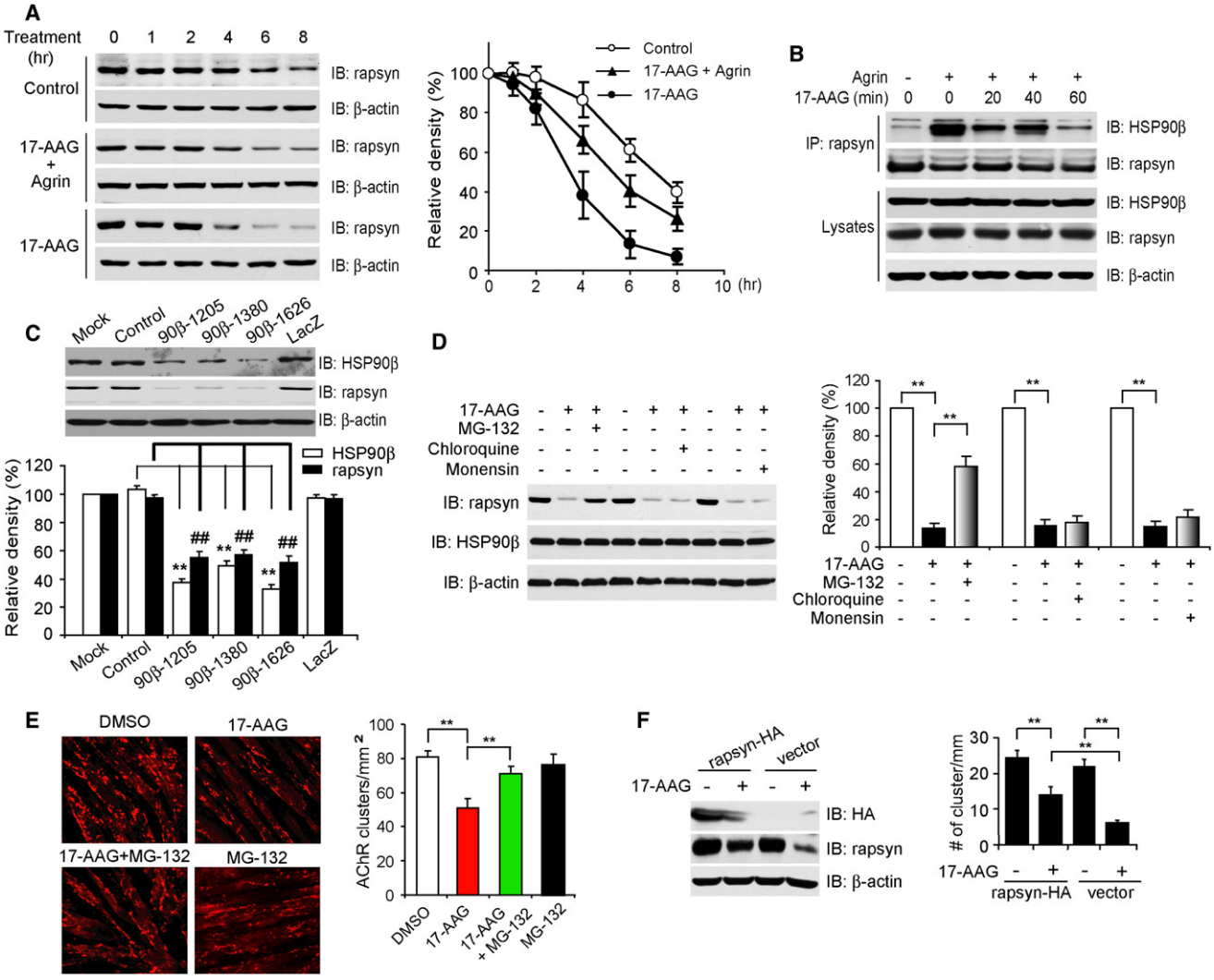

Figure 7. Regulation of Rapsyn Stability by HSP90β

(A) Reduction of rapsyn in 17-AAG-treated muscle cells. C2C12 myotubes were treated with CHX (50 μg/ml) alone or together with 17-AAG (5 μM) for the indicated times. Lysates were probed for rapsyn and β-actin (as control). Blots were scanned with an Epson scanner and analyzed by NIH Image software. Quantitative analysis was shown in the graph on the right.

(B) 17-AAG disrupted the HSP90β-rapsyn interaction. C2C12 myotubes were treated with 17-AAG (5 μM) together with or without agrin for the indicated times. The interaction was examined by coimmunoprecipitation as in Figure 2. Lysate inputs were probed with the indicated antibodies to show expression of interested proteins.

(C) HSP90β depletion by miRNA facilitated rapsyn degradation. C2C12 myotubes were transfected with the control vector, LacZ-miRNA, or HSP90β miRNA constructs and lysed 36 hr later. Rapsyn in lysates was revealed by immunoblotting with indicated antibodies. Band density was quantified and shown in the histograms. Data were shown as mean ± SEM; n = at least 5 for each data point; ** or ##, $p < 0.01$.

(D) Rapsyn reduction by 17-AAG was inhibited by MG-132, but not by lysosomal protease inhibitors. C2C12 myotubes were treated with vehicle (DMSO) or 17-AAG (5 μM) for 8 hr, with or without 10 μM MG-132, 10 mM chloroquine, or 10 mM monensin. In order to decrease toxicity, MG-132, chloroquine or monensin was added 4 hr before cell harvest. Lysates were subjected to immunoblotting with indicated antibodies. Quantitative analysis of results was shown in histograms (mean ± SEM, n = 4; **$p < 0.01$).

(E) MG-132 attenuated 17-AAG-induced inhibition of AChR cluster formation. C2C12 myotubes were treated with agrin together with DMSO, 17-AAG (1 μM), MG-132 (5 μM), or 17-AAG plus MG-132. AChR clusters were assayed as in Figure 3. Shown were mean ± SEM, n = 5; **$p < 0.01$.

(F) Overexpression of rapsyn attenuated the inhibitory effect of 17-AAG on AChR clusters. C2C12 myotubes were transfected with the empty vector or rapsyn-HA. Thirty-six hours after transfection, cells were stimulated with agrin in the presence of DMSO or 5 μM 17-AAG. Lysates were probed with antibody against rapsyn, the HA tag, or β-actin (left panel). AChR clusters were examined in HA-positive myotubes in parallel experiments (right panel). Data were shown as mean ± SEM, n = 15 each group; **$p < 0.01$.

associated with spontaneous AChR clusters was at low levels that could not be revealed by immunostaining. Nevertheless, these results suggest that HSP90β regulates agrin-regulated AChR clusters. This notion is supported by increased association of HSP90β with clustered AChR (Figure 1C, 1E, and 3B).

HSP90β is a molecular chaperone that aids in the folding, assembly-disassembly, and activation of a wide range of substrate or client proteins (Pearl and Prodromou, 2006). Many proteins are known to be enriched at the NMJ, including MuSK (DeChiara et al., 1996; Sanes and Lichtman, 2001), and in particular, several have been identified to associate with the AChR of adult rabbit muscle cells or in cultured muscle cells, including APC, actin, and α-actinin (Mitsui et al., 2000; Wang et al., 2003) (data not shown). We show that HSP90β is recruited to the AChR complex upon agrin stimulation via direct interaction with rapsyn. Inhibition of HSP90β function by 17-AAG or by a dominant-negative mutant or suppression of HSP90β expression by miRNA reduces static levels of rapsyn and its half-life in myotubes. Moreover, rapsyn levels were reduced in muscles that expressed HSP90β-miRNA or the dominant-negative mutant or in muscles from mice that were injected with 17-AAG. These results suggest that HSP90β stabilizes rapsyn and subsequently AChR clustering. Intriguingly, pretreatment of myotubes with 17-AAG also inhibited agrin-induced formation of AChR clusters. This is probably because that the inhibition of HSP90β by 17-AAG is long-lasting. A recent study indicates that 17-AAG accumulates in cells and its intracellular concentration remains high even 72 hr after treatment (Chiosis et al., 2003). Interestingly, agrin stimulation did not have consistent effect on total levels of rapsyn in muscle cells, which could suggest that HSP90β alone is not sufficient for rapsyn folding or stabilization. In support of this notion was that HSP90β overexpression had no consistent effect on levels of rapsyn or its half-life (Figure S12). These observations suggest the existence of additional mechanisms for rapsyn stabilization. In addition to HSP90β, rapsyn also associates with HSP70, another component of the HSP complex (Figures 2A and 2C). HSP70 is known to participate to regulate protein folding and degradation (Bukau and Horwich, 1998; Hartl and Hayer-Hartl, 2002). It is likely that HSP70 participates in rapsyn folding and stabilization.

It is worth pointing out that phenotypes of in vivo HSP90β inhibition were not identical to those observed in rapsyn mutant mice (Gautam et al., 1995). Postsynaptically, junctional AChR clusters appeared fragmented, in addition to expected reduction in AChR intensity, in muscles injected with 17-AAG or expressing the dominant-negative mutant or HSP90β-miRNA (Figures 4C, 6D, and 5E). Furthermore, in vitro studies showed that some AChR clusters disappeared whereas others reduced in intensity in myotubes (Figure S6 time lapse). This binary effect and fragmentation of AChR clusters could suggest a regulatory role of HSP90β in the stabilization of clusters or the NMJ, the underlying mechanisms of which, however, warrant further investigation. It is possible that HSP90β may regulate the function or stability of other proteins in addition to rapsyn. Candidates on this list include α-dystrobrevin and α-syntrophin, which have been shown to regulate the stabilization of AChR clusters (Adams et al., 2000; Banks et al., 2003; Grady et al., 2000; Pawlikowski and Maimone, 2008; Sadasivam et al., 2005). In rapsyn mutant mice, motor axons grow excessively over the entire muscle with little presynaptic differentiation (Gautam et al., 1995). However, nerve branches in 17-AAG-treated animals appeared to be similar to those in control mice (Figure 4A and 4A′). The lack of presynaptic phenotypes may be due to the time of 17-AAG injection, i.e., E14.5, being after the formation of primitive AChR clusters (Lin et al., 2001; Yang et al., 2001) and incomplete ablation of AChR clusters. It is also possible that HSP90β inhibition reduces axon mobility or suppresses expression of axon attractive molecules or trophic factors in muscles.

HSP90β inhibition did not appear to alter the levels of MuSK that is enriched in the postsynaptic membrane (Figures 3C and 3E). No consistent effect of HSP90β inhibition was observed on expression of signaling molecules that have been implicated in AChR clustering, including Abl, Rac, and Cdc42 (Figure 3D) or myosin heavy chain (MHC), MyoD, or myogenin (Figure S7A). These observations indicate the specificity of HSP90β-dependent protein stability, suggesting the necessity of direct interaction for HSP90β regulation. Rapsyn has been shown to confer AChR stability (Banks et al., 2003; Willmann and Fuhrer, 2002). However, AChR is much more stable than rapsyn, with a half-life of ~24 hr in muscle cells (Berg and Hall, 1975; Devreotes and Fambrough, 1975; Gervasio and Phillips, 2005; Wang et al., 1999). The receptor becomes more stable when clustered or at the NMJ, with a half-life of ~10 days (Levitt et al., 1980; Salpeter and Loring, 1985). Therefore, we anticipate reduced levels of AChR after long-term inhibition of HSP90β.

HSP90 has three regions: N-terminal nucleotide binding pocket for ATP and geldanamycin, the middle region for substrate/client proteins, and the C-terminal region that interact with cochaperone proteins such as HSP70, HSP40, and p23 (Pearl and Prodromou, 2006). The interaction with the cochaperones has been shown to regulate proper folding or function of substrate proteins. In line with this notion, we found that the C-terminal truncation mutant of HSP90β1-620 was unable to maintain rapsyn stability, although it was able to bind with rapsyn (Figures 2E). In fact, due to its ability to interact with rapsyn, expressed HSP90β1-620 attenuates the interaction of endogenous rapsyn and HSP90β and thus inhibits agrin-induced AChR cluster formation. These results demonstrate that the C terminus of HSP90β is involved in regulating the stability of rapsyn, suggesting the possible involvement of other chaperone proteins. Note that HSP90β overexpression did not appear to alter agrin-induced AChR clusters (Figure 6B) and had no consistent effect on levels of rapsyn or its half-life (Figure S12), suggesting that the limiting factor may not be the levels of HSP90β, but the regulated interaction with rapsyn. Exactly how rapsyn is degraded after dissociation from HSP90β remains to be fully elucidated. The inhibition of 17-AAG-induced depletion of rapsyn by MG-132 suggests that degradation occurs via 26S proteasomal-dependent hydrolysis. This conclusion is further supported by our observations that the lysosomal protease inhibitors, chloroquine and monensin, had no effect on 17-AAG-induced loss of rapsyn.

In summary, this study reveals that the stability of rapsyn is critically dependent on HSP90β, highlighting a novel function of HSP90β in NMJ formation and maintenance. It also identifies a mechanism in agrin signaling for AChR clustering, i.e., by upregulating the interaction between HSP90β and rapsyn. Agrin is

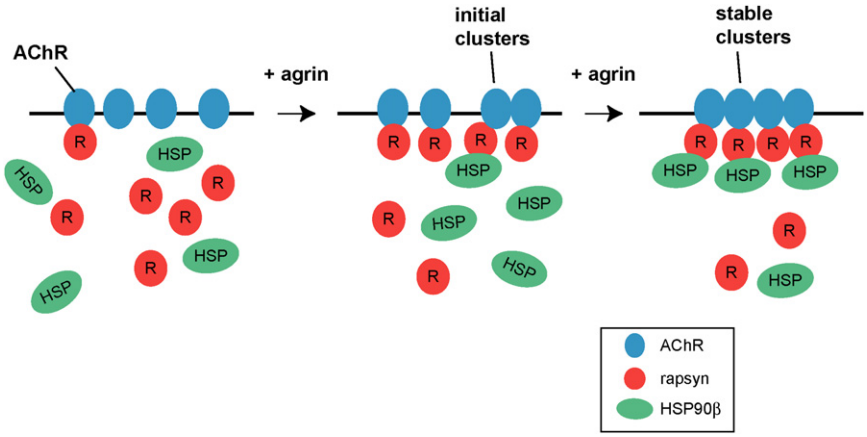

Figure 8. A Working Model
Agrin stimulates the interaction between AChR and rapsyn to initiate clustering process. Subsequently, HSP90β becomes associated with rapsyn. The latter interaction helps to stabilize rapsyn, contributing to AChR cluster formation and maintenance.

known to increase rapsyn interaction with AChR, which reaches maximal levels within 40 min of stimulation (Moransard et al., 2003). We show that levels of HSP90β in the surface AChR complex begin to increase ~1 hr after stimulation and peak around 12 hr (Figure 1C). These observations suggest that the initial targets of agrin/MuSK signaling include the interaction of the AChR and rapsyn, which is followed by the rapsyn-HSP90β association. Recruited HSP90β maintains the stability of rapsyn associated with surface AChRs, contributing to cluster formation and maintenance (Figure 8). Considering that several members of the HSP90 machinery are present at the PSD or aggresomes in neurites (Moon et al., 2001; Romorini et al., 2004; Suzuki et al., 1999; Walikonis et al., 2000), these results may provide insight into CNS synapse formation. In support of the notion, pharmacological inhibitors of HSP90 have been shown to rapidly reduce AMPA receptor currents in hippocampal slices, probably by interfering with constitutive trafficking of AMPA receptors (Gerges et al., 2004).

EXPERIMENTAL PROCEDURES

Reagents, Constructs, and Antibodies

Biotin-conjugated αBTX, R-BTX, streptavidin-coupled agarose beads, goat anti-mouse IgG conjugated with Alexa Fluor 488, donkey anti-rabbit IgG conjugated with Alexa Fluor 488, and goat anti-mouse IgG conjugated Alexa Fluor 594 were from Molecular Probes. MG-132 (Z-Leu-Leu-Leu-CHO, I-130) was from BostonBiochem. Interferon-γ was from BioSource. 17-AAG, CHX, Lubrol-PX, and other chemicals were from Sigma (St. Louis, MO). Mouse HSP90β was subcloned between EcoR V and Xho I in pcDNA-Flag, pcDNA3.1-Myc/His, or between Xho I and Sal I sites in pIRES2-EGFP (Addgene). Mouse rapsyn was subcloned between Hind III and Xba I sites in pKH3 or between EcoR I and BamH I sites in pEGFP-N1 (BD Biosciences Clontech) in-frame upstream of the GFP epitope. Rapsyn was subcloned between BamH I and EcoR I sites in pEF6/myc-his (Invitrogen) or in pGEX-2T. Respective deletion mutants were generated by using the Quick Change Site-Directed Mutagenesis Kit (Stratagene). The authenticity of all constructs was verified by DNA sequencing. The immunogen to generate the anti-HSP90β antibody was from Dr. David Toft (Mayo Clinic). GST-HSP90 mutant plasmids were a gift from Dr. Takenawa (Park et al., 2005). HSP90α- and HSP90β-miRNA constructs were generated using the BLOCK-iT Pol II miR RNAi Expression Vector Kit (Invitrogene, K4936-00). Oligonucleotide sequences for miRNA constructs were as follows: 90β-1205 5′-ATA AAG TTG AGG TAC TCA GGT-3′, for 90β-1380 5′-TTT GGA GAA GGC CTC ATA GAA-3′, for 90β-1626 5′-AAT AGG CTC AGT CAT ATA CAC-3′, for 90α-2018 5′-AAG ATG ACC AGA TCC TTC ACA-3′, for 90α-2092 5′-TGT AGA TCC TGT TAG CAT GGG-3′, for 90α-2172 5′-CAT TTC TTC AGT TAC AGC AGC-3′. Antibodies were purchased from ZYMED (HSP90β, 37-9400), Santa Cruz (HSP90α, sc-8262; HSP70, sc-24; c-Abl, sc-131; Cdc42; sc-87; MyoD, sc304; MHC, sc32732), Sigma (FlagM2, F3165), Chemicon (neurofilament, AB1983), Dako (synaptophysin, A0010), Torrey Pines Biolabs (GFP, TP401), Upstate Biotechnology (4G10, 05-321; Rac, 05-389), Novus (β-actin, NB600-501), and Abcam (myogenin, ab1835). Rabbit anti-rapsyn (2741) and anti-MuSK antibodies were described previously (Luo et al., 2002). Anti-AChR α-subunit (mAb35) and anti-AChRβ-subunit (mAb124) antibodies were gifts from Dr. Rotundo and Dr. Lindstrom, respectively. Neural agrin was prepared as described previously and used at 10 ng/ml (~0.1 nM) unless otherwise indicated (Luo et al., 2002).

Cell Culture and Transfection

Mouse muscle C2C12 myoblasts were propagated and induced to form myotubes as described previously (Luo et al., 2002). *Rapsyn*$^{-/-}$ (clone 11-7) and control (clone 12-10) myoblasts were maintained and differentiated as described previously (Zhu et al., 2006). C2C12 myoblasts were transfected with lipofectamine 2000 (Invitrogen, 11668-019) with a modified protocol. C2C12 myoblasts, at 70%–80% confluence, were rinsed once with serum-free medium before transfection because serum appeared to reduce transfection efficiency. After complete aspiration of the medium, myoblasts were incubated with a mixture of DNA, lipofectamine, and serum-free medium for 8 hr when the medium was changed to the growth medium. The DNA:lipofectamine ratio in the mixture was 1 μg:2 μl. The optimal volume of the mixture for 24-well dishes was 200 μl per well that contained 2 μg plasmid DNA. Using the modified protocol, we were able to achieve high transfection efficiency.

Isolation of Surface AChR and Associated Proteins

Myotubes were stimulated without or with agrin at 37°C for the indicated times and incubated live with 300 nM biotin-αBTX for 2 hr at 4°C. After washing, cells were lysed in the extraction buffer containing 0.5% Lubrol-PX, 50 mM KCl, 2 mM $CaCl_2$, 4 mM $MgCl_2$, 20% glycerol, 50 mM Tris-HCl, and inhibitors of proteases and phosphatases, pH 7.4. Lysates were incubated with streptavidin-coupled agarose beads for 6 hr at 4°C and washed extensively with the extraction buffer, except that the concentration of Lubrol-PX was 0.1%. Bead-associated proteins were resolved by SDS-PAGE. Bands were excised from gels, cut into 1 mm pieces, washed in 20 mM AMBIC, dried, and digested overnight in trypsin. Peptides were extracted using 5% FA in 50% CAN and were dried. Using a 1:1 dilution of CHCA matrix in 5%FA/50% ACN, samples were spotted to an ABI 4700 Proteomics Analyzer (Applied Biosystems) MALDI-ToF target plate. Four thousand shots were fired to acquire the initial MS spectrum, and the top 20 most intense peaks were selected for MS/MS analysis. Obtained sequences were used for database search with FASTA and BLAST program.

Immunoprecipitation, Immunoblotting, and In Vitro Protein Interactions

Cell lysates were cleaned by centrifugation at 12,000 rpm for 10 min and subjected to immunoprecipitation with indicated antibodies and protein-A or protein-G beads (Roche) at 4°C overnight. Bound proteins were resolved by SDS-PAGE and analyzed by immunoblotting as described previously (Luo et al., 2002; Zhu et al., 2006). In some experiments, membranes were stripped and reblotted with different antibodies as described (Luo et al., 2002; Zhu et al.,

2006). Quantification of immunoblots was done by scanning films containing nonsaturated signals with an Epson 1680 scanner and analyzed with NIH Image.

GST-rapsyn proteins were produced in BL21, purified, and immobilized on glutathione Sepharose 4B beads (Amersham Pharmacia). They were incubated with cell lysates in pull-down experiments. To assay the direct interaction, GST-HSP90β proteins were produced in BL21, purified, and immobilized on beads. [^{35}S]-labeled rapsyn was generated by in vitro translation in the presence of [^{35}S]methionine using TnT T7/SP6 Coupled Reticulocyte Lysate System (Promega) (Luo et al., 2002) and was incubated with immobilized GST-HSP90β in the binding buffer (25 mM HEPES, 1 mM DTT, 0.5% Triton X-100, and 150 mM NaCl and protease inhibitors, pH7.5) for 2 hr at 4°C on a rotator. After washing with PBS/0.1% Tween 20, bound [^{35}S]-labeled proteins were resolved on SDS-PAGE and subjected to autoradiogram.

AChR Cluster Assays

AChR clusters in C2C12 myotubes were measured as described previously (Luo et al., 2002; Zhu et al., 2006). In some experiments, young myotubes (2 days after changing to the differentiation medium) were transfected with indicated constructs using the lipofectamine 2000 kit according to the manufacturer's instruction. 24–36 hr later, transfected myotubes were subjected to AChR cluster assays. For a particular treatment, at least 20 pictures were taken from several chamber slides. AChR clusters whose diameters or longer axis was equal to or greater than 4 μm were scored with Metamorph software.

17-AAG Injection

C57BL/6J mice were injected intraperitoneally at P7, P14, and P30 with 50 μl of 17-AAG (2.5 mg/kg) three times a week for 2 weeks. Control mice received equal volumes of DMSO. AChR clusters were visualized in single teased fibers of tibialis anterior muscles, and Z serial images were collected and collapsed into a single image. Mouse embryos in uterus (E14.5) were injected intraperitoneally with 17-AAG (10 μl, 0.5 μM in 10% DMSO), returned to the pregnant mice, and injected again at E15.5. Control embryos were injected with equal volumes of the vehicle DMSO (10%). Two days after second injection, embryos (E17.5) were dissected and processed for AChR staining as described previously (Dong et al., 2006; Li et al., 2008; Zhu et al., 2006).

Intramuscular DNA Injection and Electroporation

In vivo electroporation was performed as previously described (Aihara and Miyazaki, 1998) with modification. Briefly, 14-day-old C57BL/6J mice were anesthetized with isoflurane. Respective miRNA were injected into the tibialis anterior muscles (5 μg DNA in 10 μl TE buffer). Contralateral muscles were injected with control plasmids that encode scrambled sequence. A pair of electrode needles with a 5 mm gap was inserted into the muscle to encompass the DNA injection sites, and electric pulses were delivered using an electric pulse generator (ECM830; BTX). Five pulses followed by five additional pulses of the opposite polarity were administered to each injection site. The parameters of the pulses were 50 V at 60 Hz with each pulse lasting for 50 ms. Fourteen days after electroporation, mice were sacrificed, and the tibialis anterior muscles were fixed in cold 4% PFA-PBS for 24 hr and stained with R-BTX. Individual muscle fibers were isolated and examined for AChR clusters under a Zeiss confocal laser-scanning microscope. Z serial images were collected and collapsed into a single image. AChR clusters on EGFP-positive fibers were analyzed with LSM 5 Image Examiner (Zeiss).

Statistical Analysis

Data of multiple groups were analyzed by ANOVA, followed by a student-Newman-Keuls test. Two-tailed Student's t test was used to compare data between two groups. Differences were considered significant at $p < 0.05$. Values and error bars in figures denote mean ± SEM.

SUPPLEMENTAL DATA

The Supplemental Data include Supplemental Figures and can be found with this article online at http://www.neuron.org/supplemental/S0896-6273(08)00708-3.

ACKNOWLEDGMENTS

We thank Dr. Tadaomi Takenawa for HSP90 constructs, Dr. David Toft for HSP90β protein, Dr. Rick Rotundo and Dr. Jon Lindstrom for AChR antibodies, Dr. Ezekiel Carpenter-Hyland for assistance with imaging analysis, Ms. Hannah Neiswender for technical assistance, and Mr. Eric Miller and the Proteomics Core of Medical College of Georgia for assistance with proteomics analysis. This work is support in part by grants from NIH (L.M. and W.C.X) and Muscular Dystrophy Association (L.M.).

Accepted: August 10, 2008
Published: October 8, 2008

REFERCENES

Adams, M.E., Kramarcy, N., Krall, S.P., Rossi, S.G., Rotundo, R.L., Sealock, R., and Froehner, S.C. (2000). Absence of alpha-syntrophin leads to structurally aberrant neuromuscular synapses deficient in utrophin. J. Cell Biol. *150*, 1385–1398.

Aihara, H., and Miyazaki, J. (1998). Gene transfer into muscle by electroporation in vivo. Nat. Biotechnol. *16*, 867–870.

Akaaboune, M., Culican, S.M., Turney, S.G., and Lichtman, J.W. (1999). Rapid and reversible effects of activity on acetylcholine receptor density at the neuromuscular junction in vivo. Science *286*, 503–507.

Apel, E.D., Glass, D.J., Moscoso, L.M., Yancopoulos, G.D., and Sanes, J.R. (1997). Rapsyn is required for MuSK signaling and recruits synaptic components to a MuSK-containing scaffold. Neuron *18*, 623–635.

Banks, G.B., Fuhrer, C., Adams, M.E., and Froehner, S.C. (2003). The postsynaptic submembrane machinery at the neuromuscular junction: requirement for rapsyn and the utrophin/dystrophin-associated complex. J. Neurocytol. *32*, 709–726.

Bartoli, M., Ramarao, M.K., and Cohen, J.B. (2001). Interactions of the rapsyn RING-H2 domain with dystroglycan. J. Biol. Chem. *276*, 24911–24917.

Berg, D.K., and Hall, Z.W. (1975). Loss of alpha-bungarotoxin from junctional and extrajunctional acetylcholine receptors in rat diaphragm muscle in vivo and in organ culture. J. Physiol. *252*, 771–789.

Brandon, E.P., Lin, W., D'Amour, K.A., Pizzo, D.P., Dominguez, B., Sugiura, Y., Thode, S., Ko, C.P., Thal, L.J., Gage, F.H., and Lee, K.F. (2003). Aberrant patterning of neuromuscular synapses in choline acetyltransferase-deficient mice. J. Neurosci. *23*, 539–549.

Bruneau, E., and Akaaboune, M. (2007). The dynamics of the rapsyn scaffolding protein at individual acetylcholine receptor clusters. J. Biol. Chem. *282*, 9932–9940.

Bukau, B., and Horwich, A.L. (1998). The Hsp70 and Hsp60 chaperone machines. Cell *92*, 351–366.

Camilleri, A.A., Willmann, R., Sadasivam, G., Lin, S., Ruegg, M.A., Gesemann, M., and Fuhrer, C. (2007). Tyrosine phosphatases such as SHP-2 act in a balance with Src-family kinases in stabilization of postsynaptic clusters of acetylcholine receptors. BMC Neurosci. *8*, 46.

Chen, F., Qian, L., Yang, Z.H., Huang, Y., Ngo, S.T., Ruan, N.J., Wang, J., Schneider, C., Noakes, P.G., Ding, Y.Q., et al. (2007). Rapsyn interaction with calpain stabilizes AChR clusters at the neuromuscular junction. Neuron *55*, 247–260.

Chiosis, G., Huezo, H., Rosen, N., Mimnaugh, E., Whitesell, L., and Neckers, L. (2003). 17AAG: low target binding affinity and potent cell activity–finding an explanation. Mol. Cancer Ther. *2*, 123–129.

Collingridge, G.L., Isaac, J.T., and Wang, Y.T. (2004). Receptor trafficking and synaptic plasticity. Nat. Rev. Neurosci. *5*, 952–962.

DeChiara, T.M., Bowen, D.C., Valenzuela, D.M., Simmons, M.V., Poueymirou, W.T., Thomas, S., Kinetz, E., Compton, D.L., Rojas, E., Park, J.S., et al. (1996). The receptor tyrosine kinase MuSK is required for neuromuscular junction formation in vivo. Cell *85*, 501–512.

Devreotes, P.N., and Fambrough, D.M. (1975). Acetylcholine receptor turnover in membranes of developing muscle fibers. J. Cell Biol. *65*, 335–358.

Dong, X.P., Li, X.M., Gao, T.M., Zhang, E.E., Feng, G.S., Xiong, W.C., and Mei, L. (2006). Shp2 is dispensable in the formation and maintenance of the neuromuscular junction. Neurosignals *15*, 53–63.

Elias, G.M., Funke, L., Stein, V., Grant, S.G., Bredt, D.S., and Nicoll, R.A. (2006). Synapse-specific and developmentally regulated targeting of AMPA receptors by a family of MAGUK scaffolding proteins. Neuron *52*, 307–320.

Ferns, M., Deiner, M., and Hall, Z. (1996). Agrin-induced acetylcholine receptor clustering in mammalian muscle requires tyrosine phosphorylation. J. Cell Biol. *132*, 937–944.

Finn, A.J., Feng, G., and Pendergast, A.M. (2003). Postsynaptic requirement for Abl kinases in assembly of the neuromuscular junction. Nat. Neurosci. *6*, 717–723.

Frail, D.E., Musil, L.S., Buonanno, A., and Merlie, J.P. (1989). Expression of RAPsyn (43K protein) and nicotinic acetylcholine receptor genes is not coordinately regulated in mouse muscle. Neuron *2*, 1077–1086.

Fu, A.K., Cheung, Z.H., and Ip, N.Y. (2008). Beta-catenin in reverse action. Nat. Neurosci. *11*, 244–246.

Fuhrer, C., Gautam, M., Sugiyama, J.E., and Hall, Z.W. (1999). Roles of rapsyn and agrin in interaction of postsynaptic proteins with acetylcholine receptors. J. Neurosci. *19*, 6405–6416.

Gautam, M., Noakes, P.G., Mudd, J., Nichol, M., Chu, G.C., Sanes, J.R., and Merlie, J.P. (1995). Failure of postsynaptic specialization to develop at neuromuscular junctions of rapsyn-deficient mice. Nature *377*, 232–236.

Gautam, M., Noakes, P.G., Moscoso, L., Rupp, F., Scheller, R.H., Merlie, J.P., and Sanes, J.R. (1996). Defective neuromuscular synaptogenesis in agrin-deficient mutant mice. Cell *85*, 525–535.

Gerges, N.Z., Tran, I.C., Backos, D.S., Harrell, J.M., Chinkers, M., Pratt, W.B., and Esteban, J.A. (2004). Independent functions of hsp90 in neurotransmitter release and in the continuous synaptic cycling of AMPA receptors. J. Neurosci. *24*, 4758–4766.

Gervasio, O.L., and Phillips, W.D. (2005). Increased ratio of rapsyn to ACh receptor stabilizes postsynaptic receptors at the mouse neuromuscular synapse. J. Physiol. *562*, 673–685.

Glass, D.J., Bowen, D.C., Stitt, T.N., Radziejewski, C., Bruno, J., Ryan, T.E., Gies, D.R., Shah, S., Mattsson, K., Burden, S.J., et al. (1996). Agrin acts via a MuSK receptor complex. Cell *85*, 513–523.

Grady, R.M., Zhou, H., Cunningham, J.M., Henry, M.D., Campbell, K.P., and Sanes, J.R. (2000). Maturation and maintenance of the neuromuscular synapse: genetic evidence for roles of the dystrophin-glycoprotein complex. Neuron *25*, 279–293.

Hartl, F.U., and Hayer-Hartl, M. (2002). Molecular chaperones in the cytosol: from nascent chain to folded protein. Science *295*, 1852–1858.

Herbst, R., and Burden, S.J. (2000). The juxtamembrane region of MuSK has a critical role in agrin-mediated signaling. EMBO J. *19*, 67–77.

Kim, S., and Nelson, P.G. (2000). Involvement of calpains in the destabilization of the acetylcholine receptor clusters in rat myotubes. J. Neurobiol. *42*, 22–32.

Kim, N., and Burden, S.J. (2008). MuSK controls where motor axons grow and form synapses. Nat. Neurosci. *11*, 19–27.

Levitt, T.A., Loring, R.H., and Salpeter, M.M. (1980). Neuronal control of acetylcholine receptor turnover rate at a vertebrate neuromuscular junction. Science *210*, 550–551.

Li, X.M., Dong, X.P., Luo, S.W., Zhang, B., Lee, D.H., Ting, A.K., Neiswender, H., Kim, C.H., Carpenter-Hyland, E., Gao, T.M., et al. (2008). Retrograde regulation of motoneuron differentiation by muscle beta-catenin. Nat. Neurosci. *11*, 262–268.

Lin, W., Burgess, R.W., Dominguez, B., Pfaff, S.L., Sanes, J.R., and Lee, K.F. (2001). Distinct roles of nerve and muscle in postsynaptic differentiation of the neuromuscular synapse. Nature *410*, 1057–1064.

Lin, W., Dominguez, B., Yang, J., Aryal, P., Brandon, E.P., Gage, F.H., and Lee, K.F. (2005). Neurotransmitter acetylcholine negatively regulates neuromuscular synapse formation by a Cdk5-dependent mechanism. Neuron *46*, 569–579.

Luo, Z.G., Wang, Q., Zhou, J.Z., Wang, J., Luo, Z., Liu, M., He, X., Wynshaw-Boris, A., Xiong, W.C., Lu, B., and Mei, L. (2002). Regulation of AChR clustering by Dishevelled interacting with MuSK and PAK1. Neuron *35*, 489–505.

Luo, Z.G., Je, H.S., Wang, Q., Yang, F., Dobbins, G.C., Yang, Z.H., Xiong, W.C., Lu, B., and Mei, L. (2003). Implication of geranylgeranyltransferase I in synapse formation. Neuron *40*, 703–717.

McMahan, U.J., Horton, S.E., Werle, M.J., Honig, L.S., Kroger, S., Ruegg, M.A., and Escher, G. (1992). Agrin isoforms and their role in synaptogenesis. Curr. Opin. Cell Biol. *4*, 869–874.

Misgeld, T., Burgess, R.W., Lewis, R.M., Cunningham, J.M., Lichtman, J.W., and Sanes, J.R. (2002). Roles of neurotransmitter in synapse formation: development of neuromuscular junctions lacking choline acetyltransferase. Neuron *36*, 635–648.

Mitsui, T., Kawajiri, M., Kunishige, M., Endo, T., Akaike, M., Aki, K., and Matsumoto, T. (2000). Functional association between nicotinic acetylcholine receptor and sarcomeric proteins via actin and desmin filaments. J. Cell. Biochem. *77*, 584–595.

Mittaud, P., Marangi, P.A., Erb-Vogtli, S., and Fuhrer, C. (2001). Agrin-induced activation of acetylcholine receptor-bound Src family kinases requires Rapsyn and correlates with acetylcholine receptor clustering. J. Biol. Chem. *276*, 14505–14513.

Mohamed, A.S., Rivas-Plata, K.A., Kraas, J.R., Saleh, S.M., and Swope, S.L. (2001). Src-class kinases act within the agrin/MuSK pathway to regulate acetylcholine receptor phosphorylation, cytoskeletal anchoring, and clustering. J. Neurosci. *21*, 3806–3818.

Moon, I.S., Park, I.S., Schenker, L.T., Kennedy, M.B., Moon, J.I., and Jin, I. (2001). Presence of both constitutive and inducible forms of heat shock protein 70 in the cerebral cortex and hippocampal synapses. Cereb. Cortex *11*, 238–248.

Moransard, M., Borges, L.S., Willmann, R., Marangi, P.A., Brenner, H.R., Ferns, M.J., and Fuhrer, C. (2003). Agrin regulates rapsyn interaction with surface acetylcholine receptors, and this underlies cytoskeletal anchoring and clustering. J. Biol. Chem. *278*, 7350–7359.

Okada, K., Inoue, A., Okada, M., Murata, Y., Kakuta, S., Jigami, T., Kubo, S., Shiraishi, H., Eguchi, K., Motomura, M., et al. (2006). The muscle protein Dok-7 is essential for neuromuscular synaptogenesis. Science *312*, 1802–1805.

Park, S.J., Suetsugu, S., and Takenawa, T. (2005). Interaction of HSP90 to N-WASP leads to activation and protection from proteasome-dependent degradation. EMBO J. *24*, 1557–1570.

Pawlikowski, B.T., and Maimone, M.M. (2008). alpha-Dystrobrevin isoforms differ in their colocalization with and stabilization of agrin-induced acetylcholine receptor clusters. Neuroscience *154*, 582–594.

Pearl, L.H., and Prodromou, C. (2006). Structure and mechanism of the Hsp90 molecular chaperone machinery. Annu. Rev. Biochem. *75*, 271–294.

Qu, Z., and Huganir, R.L. (1994). Comparison of innervation and agrin induced tyrosine phosphorylation of the acetylcholine receptor. J. Neurosci. *14*, 6834–6841.

Romorini, S., Piccoli, G., Jiang, M., Grossano, P., Tonna, N., Passafaro, M., Zhang, M., and Sala, C. (2004). A functional role of postsynaptic density-95-guanylate kinase-associated protein complex in regulating Shank assembly and stability to synapses. J. Neurosci. *24*, 9391–9404.

Sadasivam, G., Willmann, R., Lin, S., Erb-Vogtli, S., Kong, X.C., Ruegg, M.A., and Fuhrer, C. (2005). Src-family kinases stabilize the neuromuscular synapse in vivo via protein interactions, phosphorylation, and cytoskeletal linkage of acetylcholine receptors. J. Neurosci. *25*, 10479–10493.

Salpeter, M.M., and Loring, R.H. (1985). Nicotinic acetylcholine receptors in vertebrate muscle: properties, distribution and neural control. Prog. Neurobiol. *25*, 297–325.

Sanes, J.R., and Lichtman, J.W. (2001). Induction, assembly, maturation and maintenance of a postsynaptic apparatus. Nat. Rev. Neurosci. *2*, 791–805.

Schaeffer, L., de Kerchove d'Exaerde, A., and Changeux, J.P. (2001). Targeting transcription to the neuromuscular synapse. Neuron *31*, 15–22.

Sharp, S., and Workman, P. (2006). Inhibitors of the HSP90 molecular chaperone: current status. Adv. Cancer Res. *95*, 323–348.

Stebbins, C.E., Russo, A.A., Schneider, C., Rosen, N., Hartl, F.U., and Pavletich, N.P. (1997). Crystal structure of an Hsp90-geldanamycin complex: targeting of a protein chaperone by an antitumor agent. Cell *89*, 239–250.

Suzuki, T., Usuda, N., Murata, S., Nakazawa, A., Ohtsuka, K., and Takagi, H. (1999). Presence of molecular chaperones, heat shock cognate (Hsc) 70 and heat shock proteins (Hsp) 40, in the postsynaptic structures of rat brain. Brain Res. *816*, 99–110.

Waites, C.L., Craig, A.M., and Garner, C.C. (2005). Mechanisms of vertebrate synaptogenesis. Annu. Rev. Neurosci. *28*, 251–274.

Walikonis, R.S., Jensen, O.N., Mann, M., Provance, D.W., Jr., Mercer, J.A., and Kennedy, M.B. (2000). Identification of proteins in the postsynaptic density fraction by mass spectrometry. J. Neurosci. *20*, 4069–4080.

Wallace, B.G. (1988). Regulation of agrin-induced acetylcholine receptor aggregation by Ca++ and phorbol ester. J. Cell Biol. *107*, 267–278.

Wallace, B.G. (1991). The mechanism of agrin-induced acetylcholine receptor aggregation. Philos. Trans. R Soc. Lond. B Biol. Sci. *331*, 273–280.

Wang, Z.Z., Mathias, A., Gautam, M., and Hall, Z.W. (1999). Metabolic stabilization of muscle nicotinic acetylcholine receptor by rapsyn. J. Neurosci. *19*, 1998–2007.

Wang, J., Jing, Z., Zhang, L., Zhou, G., Braun, J., Yao, Y., and Wang, Z.Z. (2003). Regulation of acetylcholine receptor clustering by the tumor suppressor APC. Nat. Neurosci. *6*, 1017–1018.

Weston, C., Yee, B., Hod, E., and Prives, J. (2000). Agrin-induced Acetylcholine Receptor Clustering Is Mediated by the Small Guanosine Triphosphatases Rac and Cdc42. J. Cell Biol. *150*, 205–212.

Weston, C., Gordon, C., Teressa, G., Hod, E., Ren, X.D., and Prives, J. (2003). Cooperative regulation by Rac and Rho of agrin-induced acetylcholine receptor clustering in muscle cells. J. Biol. Chem. *278*, 6450–6455.

Willmann, R., and Fuhrer, C. (2002). Neuromuscular synaptogenesis: clustering of acetylcholine receptors revisited. Cell. Mol. Life Sci. *59*, 1296–1316.

Yang, X., Arber, S., William, C., Li, L., Tanabe, Y., Jessell, T.M., Birchmeier, C., and Burden, S.J. (2001). Patterning of muscle acetylcholine receptor gene expression in the absence of motor innervation. Neuron *30*, 399–410.

Zhang, B., Luo, S., Dong, X.P., Zhang, X., Liu, C., Luo, Z., Xiong, W.C., and Mei, L. (2007). Beta-catenin regulates acetylcholine receptor clustering in muscle cells through interaction with rapsyn. J. Neurosci. *27*, 3968–3973.

Zhou, H., Glass, D.J., Yancopoulos, G.D., and Sanes, J.R. (1999). Distinct domains of MuSK mediate its abilities to induce and to associate with postsynaptic specializations. J. Cell Biol. *146*, 1133–1146.

Zhu, D., Xiong, W.C., and Mei, L. (2006). Lipid rafts serve as a signaling platform for nicotinic acetylcholine receptor clustering. J. Neurosci. *26*, 4841–4851.